Combination of integrated slice-specific dynamic shimming and pixel-wise unwarping of residual EPI distortions

Alto Stemmer[1] and Berthold Kiefer[1]
[1]*Healthcare, Siemens AG, Erlangen, Germany*

Target audience: Imaging scientists interested in reducing EPI distortions and signal voids.

Introduction & Purpose: Due to its short acquisition time and motion insensitivity, single-shot EPI is the most important sequence in clinical diffusion weighted imaging (DWI). The main disadvantages of EPI are distortions and signal voids in regions with local B_0 inhomogeneity. This is particularly a problem in the neck region where the B_0 field varies rapidly in the feet-to-head direction. Changing the center-frequency and the shim settings between acquisitions of different slices (dynamic shimming [1]) can reduce the problems. However, 2nd order shim channels often cannot be utilized for dynamic shimming since the shim settling times are significant longer than the time between slices. With 1st order shimming (gradient offsets) alone, it is usually not possible to compensate the B_0 offset off all pixels of a slice simultaneously. Furthermore, the different shim settings also lead to different distortions in neighboring pixels of adjacent slices so that the anatomy appears unnaturally deformed in 3D reformats of the acquired slice stack. A method to reduce distortions on a pixel scale is the field map method [2]. The field map method acquires a field map to measure the local off-resonance, which is then transformed in a pixel shift map for the purpose of unwarping the distortions during post-processing. However, the field map method cannot undo signal voids in regions where a local field gradient causes a phase change across the pixel in the order of 2π or due to other B_0-sensitive techniques like gradient reversal for fat suppression. In this work, the field map method is combined with dynamic gradient-offset shimming. The dynamic shimming avoids the most severe signal voids. The field map method is used subsequently to reduce residual distortions.

Methods: The acquisition of the field map is integrated into a single-shot EPI-DWI sequence (iShim). This non-product sequence first acquires 2D multi-echo gradient images for each imaging slice. FoV and orientation are adapted from the respective imaging slice. The echo-time difference of the first and last echo is chosen such that fat and water alias. A phase difference image is calculated from these two echoes. The remaining processing of the field map data is done in 3D and comprises phase unwrapping, background masking using the sum-of-squares magnitude image of all echoes, and a calibration to avoid global 2π offsets using the intermediate echoes.

For dynamic shimming, a 2D plane is fitted to each field map slice to determine the center frequency and gradient offsets. Center frequency and gradient offsets are then updated before the acquisition of each EPI imaging slice in real time.

A virtual residual field map is calculated by removing from each pixel of the measured field map the frequency that corresponds to the gradient offsets and the center frequency of the respective slice. This virtual field map is input to the unwarping operation which is integrated directly into the post-processing of the EPI data. The unwarping is implemented in image space. Pixels for which no field information is available (due to the aforementioned background masking) are either not corrected or also masked. The latter is in particular beneficial when MIP images are part of the post-processing like it is often the case in whole-body DWI.

The iShim works-in-progress sequence was tested in multiple volunteers and also clinically in 75 patients. The newer additional distortion correction was evaluated by reprocessing data stored from these earlier scans using the Siemens Retro-Recon feature.

Results: Fig. 1b-d compares single-shot EPI-DWI images (b=800s/mm^2) acquired at two stations in a healthy 73 year old female volunteer with a 3T Siemens MAGNETOM Skyra (maximum gradient amplitude 45 mT/m, slew rate 200 T/m/s). Each station comprises 50 axial 5mm slices with zero gap. The images shown are sagittal grey-scale-inverted thin MIPs of the composed images from both stations. Fig.1a was calculated from undistorted T2-w STIR-HASTE reference images. For the images used for Fig. 1b a conventional high-order shim was performed per station. The other two images (Fig. 1c/d) are reconstructed from the same data and were acquired with dynamic gradient offset shimming. The difference is that the reconstruction of the images used for Fig. 1d included the described unwarping. The spinal cord in Fig. 1b shows a discontinuity at the station boundary (red arrow). Additionally, the diameter of the spinal cord appears reduced in the feet-most images of the 1st station compared to the head-most images of the 2nd station. The discontinuity and the signal loss are avoided by dynamic shimming (Fig. 1c). However, the spine and also the chest wall still appear deformed compared to the reference (Fig. 1a). This deformation is greatly reduced using the combined method (Fig. 1d).

Conclusions: Dynamic gradient-offset and center frequency update avoids signal voids in the neck region, which are often observed in scans where a conventional high-order shim is performed per station. It also reduces the most severe distortions at the station boundaries, which are known as "broken-spine artefact". The usage of a virtual residual field map to reduce remaining distortions, demonstrated here, avoids unnatural deformation due to varying shim setting between slices and does not require extra measurement or significant processing time. Distortions due to eddy currents induced by switching Diffusion or EPI gradients cannot be compensated since the corresponding fields are not present during the field map acquisition.

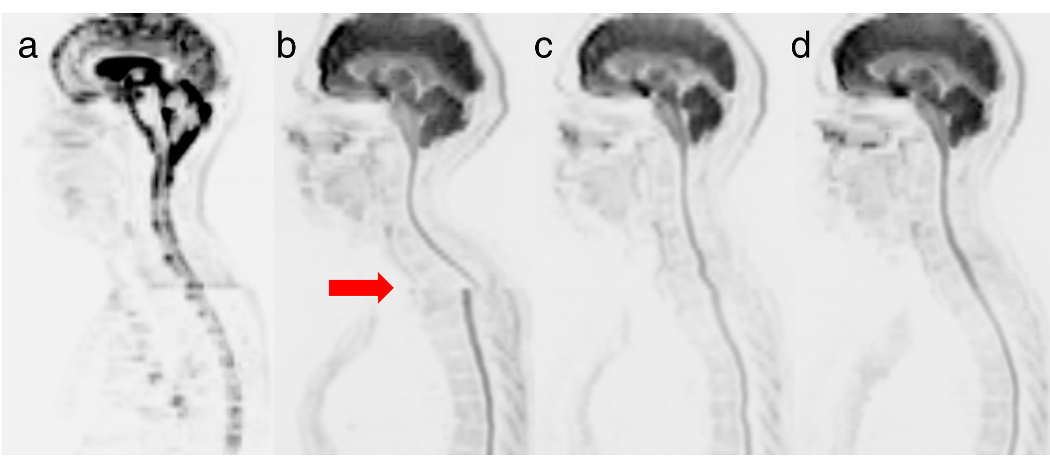

Figure 1: Sagittal thin MIP images calculated from axial images acquired at two stations: (a) T2w-STIR HASTE reference; Diffusion weighted single-shot EPI-DWI using a conventional high-order shim per station (b); dynamic 1st order shimming (c) and dynamic 1st order shimming with distortion unwarping (d), respectively.

References:

1. G. Morell and D. Spielman MRM38:477-483 (1997);

2. P. Jezzard and R.S. Balaban MRM34:65-73 (1995).